Am J Transl Res 2025;17(12):9594-9607
www.ajtr.org /ISSN:1943-8141/AJTR0169475

Original Article

Integrating flow cytometric profile and gene mutation analysis of intact lymph nodes to refine lymphoma immunophenotype

Qun-Yi Peng*, Hong-Yuan Chen*, Yan Zheng, Xiong-Peng Zhu, Chun-Tuan Li

*Department of Hematology, Quanzhou First Hospital of Affiliated to Fujian Medical University, Quanzhou 362000, Fujian, China. *Equal contributors.*

Received October 22, 2025; Accepted November 26, 2025; Epub December 15, 2025; Published December 30, 2025

Abstract: Objective: To evaluate the diagnostic use of integrating multi-parameter flow cytometry (FCM), histopathology, and gene mutation analysis for lymphoma classification using intact lymph node (LN) samples. Methods: Intact LN samples from 109 patients with lymphadenopathy were retrospectively analyzed by pathology, multi-color FCM, and next-generation sequencing (NGS) targeting 62 lymphoma-related genes. Results: FCM immunophenotyping showed high concordance with pathology (56/56 lymphoma cases detected by FCM were pathologically confirmed). PD-1 on T cells was significantly elevated in B-cell lymphoma (BCL), especially diffuse large BCL (DLBCL) (P<0.05). All BCLs exhibited monotypic intracellular cKappa or cLambda expression. Significant differences in cell size (FSC) were observed: Chronic Lymphocytic Leukemia/Small Lymphocytic Lymphoma (CLL/SLL) (mean FSC: 89.42±6.01) and Follicular Lymphoma cells (FL; 93.88±4.94) were smaller than normal B-cells (102.09±11.58), while DLBCL cells (121.84±9.17) were larger (all P<0.05). Subtypes showed distinct mutation profiles, including IGHV (9/11) in CLL/SLL; BCL2 (5/7) and EZH2 (4/7) in FL; and BCL6 (5/13) in DLBCL. Mutation-guided FCM confirmed BCL2 protein expression in two FL cases and BCL6 in one DLBCL case. T/NK-cell lymphomas showed aberrant antigen expression and restricted TRBC1 clonality (1.17%±1.61% or >96.4%) outside the normal polyclonal range (36.60%±7.21%). Conclusion: FCM on intact LNs is a robust tool with high pathologic concordance. Integrating genetic mutation data with FCM provides a powerful, multi-parameter strategy. This approach moves beyond standard immunophenotyping to include mutation-associated antigens, thereby refining lymphoma classification and enhancing diagnostic accuracy.

Keywords: Antigen expression profiles, PD-1, gene mutation, TRBC1, immunophenotype, lymph node

Introduction

Lymphoma is a highly heterogeneous hematologic malignancy with a rising incidence in China, where implementing a multi-modal diagnostic approach is not an easy task [1-3]. Diagnosis primarily relies on histopathology and immunohistochemistry (IHC) of excised lymph node [4]. Multi-parameter flow cytometry (FCM) has emerged as a potent and fast adjunct, providing quantitative, single-cell analysis essential for diagnosis, subtyping, and staging [5, 6]. Technological developments have further expanded the antibody panels available forFCM, enabling increasingly complex immunophenotyping [7, 8].

The main strength of FCM lies in its ability to rapidly detect cellular clonality, which is a hallmark distinguishing neoplastic lymphoid proliferations from reactive polyclonal processes. In most B-cell lymphomas, light-chain restriction remains a powerful indicator of clonality [9, 10]. Diagnosis of T-cell and NK-cell lymphomas is more challenging due to the absence of specific markers; these diagnoses rely largely on identifying aberrant expression of pan-T-cell antigens (CD2, CD3, CD5, CD7) and abnormal CD4/CD8 expression patterns [11, 12]. Recently, the analysis of T-cell clonality has been enhanced by a new breakthrough, namely T-cell receptor constant 1 (TRBC1) analysis by FCM [13, 14].

https://doi.org/10.62347/UECV2720

Regardless of its strength, the clinical use of FCM in the diagnosis of primary lymphoma is usually constrained by sample type. FCM is most commonly performed on peripheral blood, bone marrow, or body fluid, which are informative only when the lymphoma has disseminated or has leukemic involvement [15]. Although fine-needle aspiration (FNA) of lymph nodes is increasingly utilized, its low cellularity limits the breadth of antibody profiles that can be applied and prevents evaluation of tissue architecture, hence, hindering a complete classification [16]. Excisional lymph node biopsy remains the preferred specimen type for histopathologic assessment; however, the use of FCM on these tissues is still limited [17, 18]. Employing comprehensive FCM on single-cell suspensions derived from intact lymph nodes represents a fundamental step toward streamlining the diagnostic process.

Moreover, contemporary lymphoma diagnosis is increasingly evolving into a multimodal diagnosis encompassing morphology, immunophenotyping, and increasingly, molecular and genetic data. The 2022 World Health Organization (WHO) classification places greater emphasis on recurrent genetic abnormalities to more accurately define lymphoma subtypes [19]. Recently, genetic analysis (NGS) and immunophenotyping (FCM) are often performed as independent, parallel operations, resulting in an information gap that limits the full diagnostic potential achievable by applying these two potent technologies.

In this study, the main innovation was in addressing this gap by proposing a mutation-guided immunophenotyping strategy. We hypothesize that genetic mutation data should not be only used as a prognostic or a classification indicator, but also as a direct basis for refining FCM analysis. For example, an intracellular FCM assay should first be performed to evaluate BCL2 protein expression before the identification of a BCL2 mutation using NGS. This creates a feedback mechanism, in which the mutant (genotype) is validated at the functional protein level (phenotype), thereby refining the immunophenotypic characterization of lymphoma.

Clinically, this integrated method has the ability to provide a more potent, unified and speedy diagnostic workflow. Accordingly, this study aimed to: 1) Assess the diagnostic concordance between FCM and histopathology in intact lymph node samples; 2) characterize the informative immunophenotypic profiles and corresponding gene mutation landscapes across diverse lymphoma subtypes; and 3) demonstrate the novel application of gene mutation analysis for identifying tumor-associated antigens, enabling tailored lymphoma immunophenotyping and enhanced diagnostic accuracy.

Materials and methods

Study design and patient selection

We retrospectively reviewed the records of 152 patients with lymphadenopathy treated at Quanzhou First Hospital between January 2020 and December 2023. A total of 109 patients who underwent lymphadenectomy and had sufficient archival lymph node samples available for both flow cytometry and NGS analysis were included in the final cohort. Among them, 43 patients were excluded due to: (1) incomplete clinical data (n=18); (2) inability to obtain an intact lymph node sample (n=21); and (3) refusal to sign the informed consent form (n=4). A final cohort of 109 patients was included in this retrospective analysis (**Figure 1**).

This study adhered to the principles outlined in the Declaration of Helsinki and was approved by the Ethics Committee of Quanzhou First Hospital Affiliated to Fujian Medical University (approval number 2022106). Written informed consent was obtained from all participants or their guardians.

Inclusion criteria: Patients presenting with lymphadenopathy (>1.5 cm) confirmed by clinical examination or imaging. Exclusion criteria: (1) Patients undergoing only fine-needle aspiration (FNA) or core needle biopsy, failing to provide intact lymph nodes; (2) Samples with extensive necrosis or insufficient cellularity; (3) Patients with a definitive non-lymphoma diagnosis prior to biopsy.

Data extraction and laboratory procedures

Sample collection and histopathologic analysis: Fresh lymph node samples obtained during surgery were processed for routine pathology and flow cytometry. Residual samples were stored/banked. For this study, genetic muta-

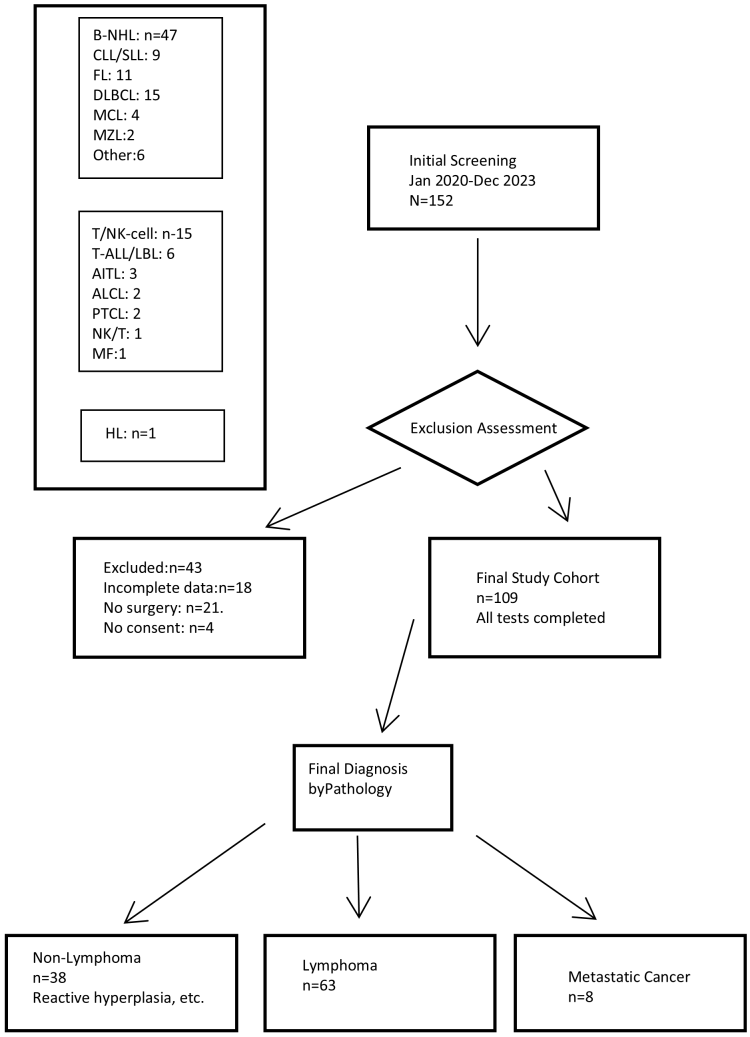

Figure 1. Flow diagram of patient selection.

tion analysis (NGS) was performed on archived DNA samples extracted from the specimens. Samples were sent for routine pathologic examinations, including H&E staining and immunohistochemistry, with diagnoses confirmed by two or more pathologists.

FCM immunophenotyping: In addition, lymph node specimens were sent to the hematology laboratory for FCM. Lymph nodes were mashed through a 200 μm nylon mesh filter (BD Falcon, USA) and centrifuged at 1000 rpm for 5 min. After discarding the supernatant, the pellet was washed three times, and a single cell suspension was prepared in normal saline at a final density of 5×10^6 cells/ml. Antibodies from the screening panel (**Table 1**) were added to 100 μl sample for 15 min. FCM analysis was performed using a Navios 3-laser 10-color flow cytometer (A53367, Beckman Coulter) and Kaluza analysis software (C00155, Beckman Coulter).

If abnormal B cells were detected, intracellular light-chain assessment was performed. Briefly, 100 μL of the sample was incubated with intracellular cKappa and cLambda antibodies for 15 min, followed by fixation with 10 μL of IntraPrep Reagent 1 (A07803, Beckman Coulter) and red blood cell lysis using 200 μL of OptiLyse C (A11894, Beckman Coulter) for 15 min. The sample was then centrifuged at 1200 rpm for 5 min, after which the supernatant was discarded. 200 μl of IntraPrep Reagent 2 (A07803, Beckman Coulter), 10 μl Kappa and 10 μl lambda were added and incubated for 20 min. Additional staining with the B-cell antibody panel was performed (**Table 1**).

All antibodies used in this study are detailed in **Table 1**. Kappa, lambda, sIgM, and terminal deoxynucleotidyl transferase (TdT) antibodies were purchased from Dako Denmark AS (Glostrup, Denmark). The TRBC1 antibody was purchased from Caprico Biotechnologies.

Antigen expression was classified according to the percentage of positively labeled cells and fluorescence intensity (Supplementary Figure 1): "-" (negative expression) if the positively labeled cell population was ≤15%; "+" (positive expression) if the positively labeled cell population was ≥70%; "+/-" (partial expression) if the positively labeled cell population was 15-70%; "++" or "+++" (strong expression) if the positively labeled cell population was ≥70% and its fluorescence intensity exceeded that of the positive control; and "dim+" (weak expression) if the exceeded population was ≥70% but its fluorescence intensity was lower than that of the positive control.

Table 1. Antibody panels used in flow cytometric immunophenotyping of lymphomas

Classification	Antibody Panel
Screening panels	CD2-FITC/CD7-PE/CD5-PC5.5/CD4-PC7/CD3-APC/CD45-KO/CD8-APCCY7
	Kappa-FITC/Lambda-PE/CD5-PC5.5/CD19-PC7/CD20-APC/CD45-KO/CD10-APCCY7
Additional panels	
B cell lymphoma	CD274-FITC/CD279-PE/CD3-PC5.5/CD19-PC7/CD56-APC/CD45-KO
	CD71-FITC/CD43-PE/CD19-PC7/CD79b-APC/CD45-KO
	FMC7-FITC/CD200-PE/CD123-PC5.5/CD19-PC7/CD23-APC/CD45-KO
	CD103-FITC/CD25-PE/CD22-PC5.5/CD19-PC7/CD11c-APC/CD45-KO
	sIgM-FITC/CD81-PE/CD38-PC5.5/CD19-PC7/IgD-APC/CD45-KO
T/NK cell lymphoma	TCR-αβ-FITC/TCR-γδ-PE/CD3-PC5.5/CD(2 OR 5 OR 7)-PC7/TRBC1-APC/CD45-KO
	CD45RA-FTIC/CD45RO-PE/CD3-PC5.5/CD(2 OR 5 OR 7)-PC7/CD30-APC/CD45-KO
	CD57-FITC/CD161-PE/CD3-PC5.5/CD(2 OR 5 OR 7)-PC7/CD94-APC/CD45-KO
	CD16-FITC/CD26-PE/CD25-PC5.5/CD(2 OR 5 OR 7)-PC7/CD3-APC/CD45-KO
	CD1A-FITC/CD99-PE/CD3-PC5.5/CD(2 OR 5 OR 7)-PC7/CD56-APC/CD45-KO
T-ALL/LBL	CD9-FITC/CD117-PE/CD33-PC5.5/HLADR-PC7/CD34-APC/CD45-KO
	CD15-FITC/CD11b-PE/CD13-PC5.5/CD16-PC7/CD34-APC/CD45-KO
	CD65-FITC/CD64-PE/CD14-PC5.5/CD4-PC7/CD34-APC/CD45-KO
	CD71-FITC/CD34-PE/CD123-PC5.5/CD61-PC7/CD36-APC/CD45-KO
	CD38-FITC/CD10-PE/CD20-PC5.5/CD19-PC7/CD34-APC/CD45-KO
	cTDT-FITC/MPO-PE/cCD3-PC5.5/CD34-PC7/CD79a-APC/CD45-KO

Genetic mutation analysis: The lymphoma samples identified by FCM were sent to Nanjing Practice Medical Diagnostics Co., Ltd. for NGS to analyze mutations in 62 genes and TCR gene rearrangement related to lymphoma (Supplementary Table 1).

Outcome measures

The primary outcome of this study was the diagnostic concordance between multi-parameter FCM and histopathologic outcome using intact excisional lymph node samples. Secondary outcome measures included: 1) Characterization and comparison of immunophenotypic profiles (e.g., cell size, antigen expression) across various lymphoma subtypes, and their associated gene mutation landscapes; and 2) Evaluation of the use of a "mutation-guided" immunophenotyping strategy, in which genetic mutations (e.g., BCL2, BCL6) were used to guide subsequent FCM analysis for corresponding protein expression, thereby refining the lymphoma classification.

Statistical analysis

Statistical analysis was performed using SPSS 25.0 (IBM Corp., USA). Categorical data were described as counts (n) and percentages (%) and compared between groups using the Pearson's χ^2 test or Fisher's exact test, as appropriate. Continuous data were first assessed for normal distribution (using the Shapiro-Wilk test) and homogeneity of variance (using Levene's test). Data conforming to a normal distribution were expressed as mean ± standard deviation (SD) and compared between groups using an independent samples t-test.

A two-tailed *P*-value <0.05 was considered significant. Data were visualized using GraphPad Prism software version 6.0 (GraphPad Software, USA), Kaluza analysis software (Beckman Coulter, USA), and FlowJo software version 10.8.1 (BD Life Sciences, USA).

Results

Clinical data

The patient selection process is detailed in **Figure 1**. Of the 109 patients with lymphadenopathy, 56 (51.38%) were male (mean age: 54 years [12-83]), and 53 (48.62%) were female (mean age: 49 years [6-83]). Lymphoma detection rates, by both FCM and pathology, were significantly higher in patients aged ≥60 years

Table 2. Clinical data

Characteristic	N	FCM	Pathology
Age			
<60 years	65	24 (38.46%)	30 (44.62%)
≥60 years	44	32 (75.00%)*	41 (86.36%)*
Sex			
Male	56	32 (58.93%)	41 (69.64%)
Female	53	24 (47.17%)	30 (52.83%)
Smoking			
Yes	15	10 (53.33%)	12 (53.33%)
No	94	46 (53.19%)	59 (62.77%)
Alcohol consumption			
Yes	11	6 (63.64%)	8 (72.73%)
No	98	50 (52.04%)	63 (62.20%)
Hepatosplenomegaly			
Yes	6	4 (66.67%)	5 (83.33%)
No	103	52 (52.43%)	66 (60.19%)
Lymph nodes excised			
Cervical	81	38 (50.62%)	48 (58.02%)
Axillary	4	3 (75.00%)	4 (100.00%)
Inguinal	10	7 (70.00%)	9 (60.00%)
Abdominal	6	5 (83.33%)	5 (83.33%)
Pharyngeal	2	1 (50.00%)	1 (100.00%)
Skin	2	1 (0.00%)	1 (100.00%)
Submandibular	2	1 (50.00%)	2 (50.00%)
Supraclavicular	2	0 (0.00%)	1 (50.00%)

*$P<0.05$. Abbreviation: FCM, flow cytometry.

Table 3. Agreement between pathology and flow cytometry in 109 lymph node samples

WHO classification	Pathology	FCM	Agreement rate (%)
CLL/SLL	9	9	100.00
FL	11	11	100.00
MCL	4	4	100.00
MZL	2	2	100.00
DLBCL	15	13	86.67
Other B cell lymphomas	6	6	100.00
T- and NK-cell lymphomas	15	11	73.33
Hodgkin lymphoma	1	0	0.00
Metastasis	8	1	12.50
Reactive	38	53	71.70

Notes: BCL, B-cell lymphoma; CLL, chronic lymphocytic leukemia; DLBCL, diffuse large B-cell lymphoma; FCM, flow cytometry; FL, follicular lymphoma; MCL, mantle cell lymphoma; MZL, marginal zone lymphoma; NK, natural killer; SLL, small lymphocytic lymphoma; WHO, World Health Organization.

compared with those aged <60 years (P<0.05). Other factors, such as sex, smoking, alcohol consumption, hepatosplenomegaly, and lymph nodes excised, were not associated with lymphoma detection (P>0.05) (**Table 2**).

Lymphoma detection by pathological findings

Pathologic analysis identified 71 patients (71/109) with abnormal lymph node findings. Of these, 47 had B-cell non-Hodgkin lymphoma (B-NHL), including 9 cases of chronic lymphocytic leukemia/small lymphocytic lymphoma (CLL/SLL), 11 of follicular lymphoma (FL), 15 of diffuse large B cell lymphoma (DLBCL), 4 of mantle cell lymphoma (MCL), 2 of marginal zone lymphoma (MZL), and 6 of other BCL. In addition, 15 had T- and NK-cell lymphoma, including 6 cases of T-ALL/LBL, 3 of angioimmunoblastic T-cell lymphoma (AITL), 2 of anaplastic large cell lymphoma (ALCL), 2 of peripheral T-cell lymphoma (PTCL), 1 of NK/T-cell lymphoma, and 1 of mycosis fungoides (MF). Besides, 1 case of Hodgkin lymphoma and 8 cases of metastasis were detected (**Table 3**).

Lymphoma detection by FCM

FCM identified 56 lymph node samples with abnormal immunophenotypic patterns, all of which were confirmed as lymphoma by pathology. Among them, 45 had B-NHL, including 9 cases of CLL/SLL, 11 of FL, 13 of DLBCL, 4 of MCL, 2 of MZL, and 6 of other BCL. In addition, 11 cases of T- and NK-cell lymphoma and 1 of metastasis were also detected (**Table 3**).

Diagnostic performance of flow cytometry

To assess the diagnostic value of FCM, its performance was compared with the gold standard, histopathology. All 109 cases were histologically categorized as either lymphoma (n=71)

Table 4. Diagnostic performance of Flow Cytometry (FCM) in detecting lymphoma using histopathology as the gold standard

	Histopathology: Positive (Lymphoma)	Histopathology: Negative (Non-Lymphoma)	Total
FCM: Positive	56 (True Positive, TP)	0 (False Positive, FP)	56
FCM: Negative	15 (False Negative, FN)	38 (True Negative, TN)	53
Total	71	38	109

Table 5. Summary of diagnostic performance metrics for FCM with 95% confidence intervals

Performance Metric	Value	95% Confidence Interval
Sensitivity	78.9% (56/71)	67.6%-87.7%
Specificity	100% (38/38)	90.8%-100%
Positive Predictive Value (PPV)	100% (56/56)	93.6%-100%
Negative Predictive Value (NPV)	71.7% (38/53)	57.7%-83.2%
Overall Accuracy	86.2% (94/109)	78.3%-92.1%
Cohen's Kappa (κ)	0.72	0.60-0.84

or non-lymphoma (n=38). The comparative results are detailed in a 2×2 contingency table (**Table 4**).

Key diagnostic performance metrics and their 95% confidence intervals (CIs) were calculated and are presented in **Table 5**. The analysis revealed that FCM had a sensitivity of 78.9% (95% CI: 67.6%-87.7%) and a specificity of 100% (95% CI: 90.8%-100%). This perfect specificity resulted in a positive predictive value (PPV) of 100% (95% CI: 93.6%-100%), indicating no false-positive results. The negative predictive value (NPV) was 71.7% (95% CI: 57.7%-83.2%). The overall diagnostic accuracy was 86.2% (95% CI: 78.3%-92.1%). Furthermore, a Cohen's Kappa (κ) coefficient of 0.72 (95% CI: 0.60-0.84) was calculated, demonstrating substantial agreement between the FCM findings and histopathologic results.

Identification of abnormal B cells by FCM and PD-1 expression

Lymphocytes were identified on the CD45 vs. side scatter (SSC) plot, following which B lymphocytes were gated on the CD19 vs. CD20 scatter plot. Abnormal B lymphocytes were defined using cKappa vs. cLambda, CD5 vs. CD20, and CD19 vs. CD10 scatter plots. Abnormal B cells generally exhibited monotypic expression of ckappa or clambda (**Figure 2A**). Regarding surface kappa/lambda detection, four cases showed no expression. Lymph node samples with abnormal B cells were further analyzed with an additional antibody panel: CD71, CD43, CD79b, FMC7, CD200, CD123, CD23, CD103, CD25, CD22, CD11c, sIgM, CD81, CD38, IgD, and CD274.

In patients with lymphoma, PD-1 (CD279) expression on T cells was increased compared to controls, most prominently in diffuse large B-cell lymphoma ($P<0.05$). This may be related to immunosuppression within the tumor microenvironment (**Figure 2B**).

CLL/SLL

CLL/SLL cells demonstrated a significantly lower mean FSC value than that of normal B lymphocyte populations (89.42±6.01 vs. 102.09±11.58, $P<0.05$), indicating that CLL/SLL cells are smaller in size (**Figure 2C**). These cells exhibited monotypic expression of ckappa or clambda. In addition, CLL/SLL cells showed strong expression of CD45 antigen, and other consistently expressed antigens included CD19, CD200, and CD5. Antigens such as CD20, CD43, CD79b, CD23, CD11c, CD22, CD81, sIgD, sIgM, and CD38 showed variable patterns (positive, weak, partial, or negative); antigens that were consistently absent included CD10, CD3, FMC7, CD56, CD8, CD71, CD123, CD103, CD25, CD4, and CD274 (**Figure 2D**). The most frequent gene mutations were primarily in IGHV (9/11), MYD88 (6/11) and KMT2C (5/11) (**Figure 2E**).

Follicular Lymphoma (FL)

FL cells demonstrated a significantly lower average FSC signal than that of normal B lymphocyte populations (93.88±4.94 vs.

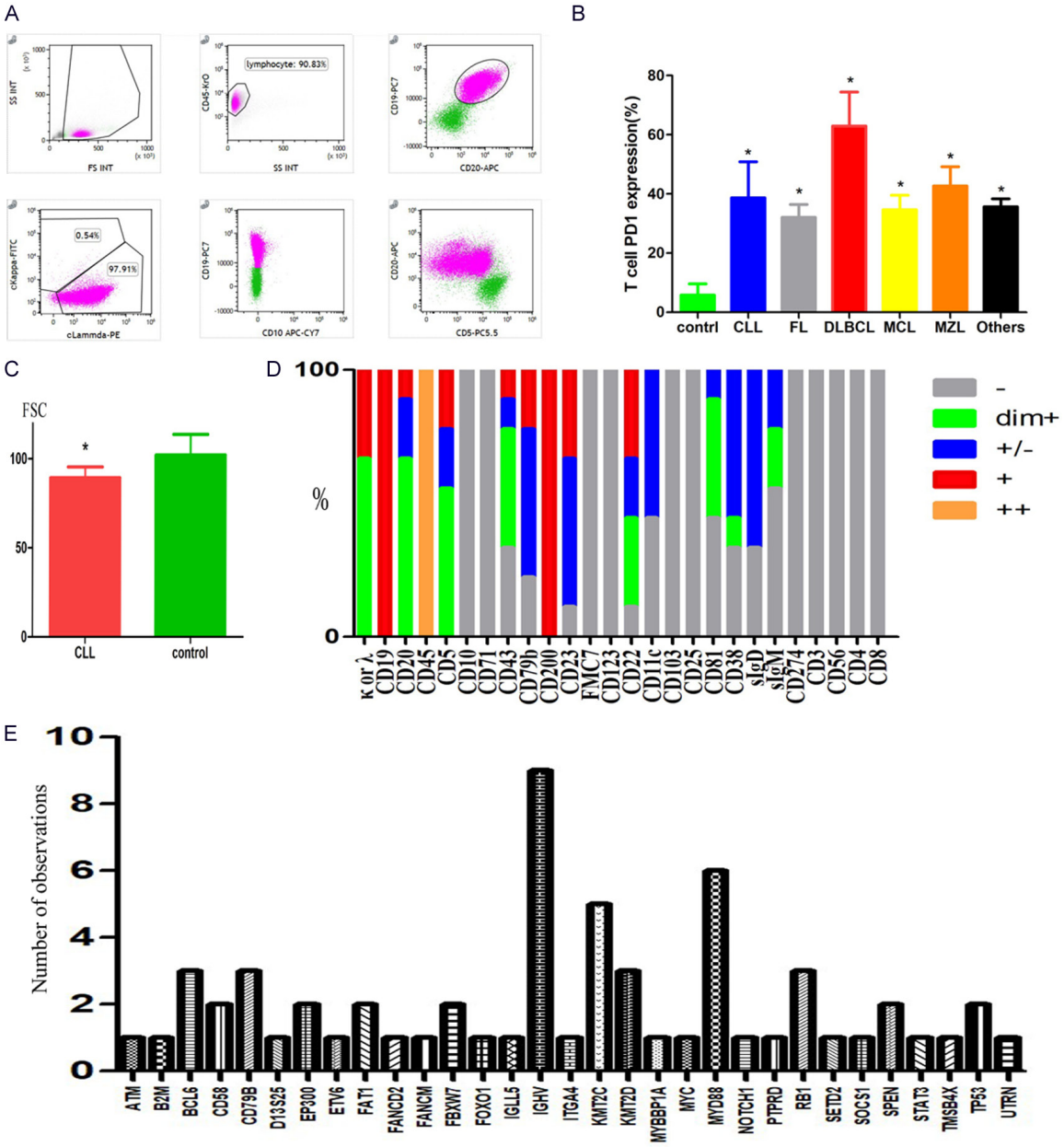

Figure 2. Flow cytometric analysis of antigen expression profiles in 9 CLL/SLL lymph node samples. A. Screening for abnormal B cells in lymph nodes. B. T cell PD-1 expression in lymphoma. C. Average FSC signal from B cells in the CLL and control groups. D. Antigen expression profiles of BCL cells in 9 CLL/SLL lymph node samples. E. Analysis of gene mutations in 9 CLL/SLL samples. BCL, B-cell lymphoma; CLL, chronic lymphocytic leukemia; SLL, small lymphocytic lymphoma; FSC, forward scatter. -, negative expression; +, positive expression; +/-, partial expression; dim+, weak expression; and ++, strong expression. *, *P<0.05*.

102.09±11.58, P<0.05), indicating its smaller cell size (**Figure 3A**). FL cells also showed monotypic expression of ckappa or clambda, and CD45 was strongly or positively expressed. CD19, CD20, CD10, CD79b, and CD22 were positively, partially, or weakly expressed. Antigens such as CD71, CD200, FMC7, CD43, CD23, CD11c, CD81, CD25, sIgD, sIgM, CD8, and CD38 showed positive, weak, partial, or no expression; antigens that were consistently absent included CD5, CD3, CD56, CD123, CD103, CD4, and CD274 (**Figure 3B**). In FL, the mutations of BCL2 (5/7) and EZH2 (4/7) were the most frequent (**Figure 3C**). Consequently,

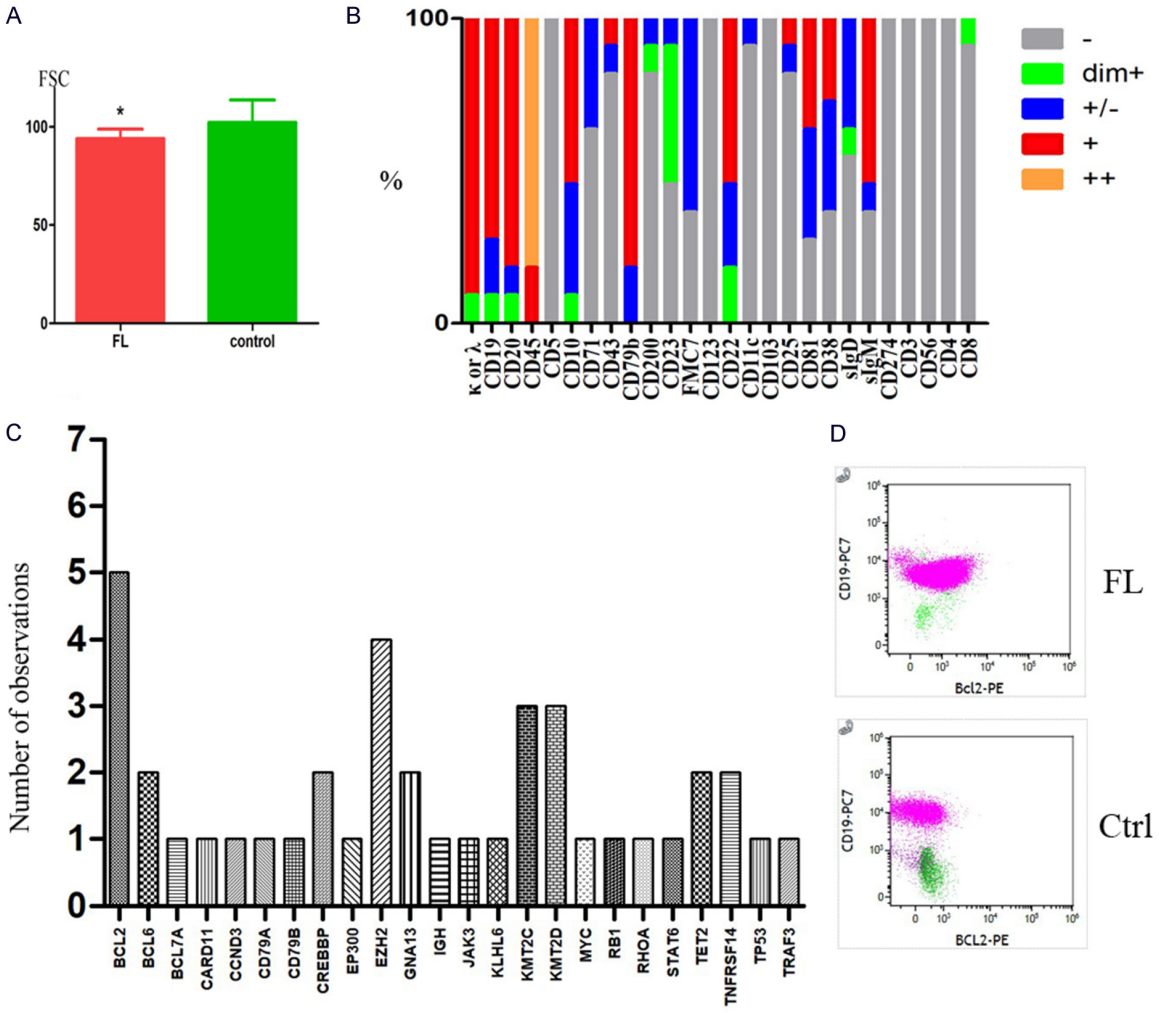

Figure 3. Flow cytometric analysis of antigen expression profiles in 11 FL lymph node samples. A. Average FSC signal from B cells in the FL and control groups. B. Immunophenotypic features of BCL cells in 11 FL lymph node samples. C. Analysis of gene mutations in 11 FL samples. D. BCL-2 expression in FL by FCM. FL, follicular lymphoma; FSC, forward scatter. -, negative expression; +, positive expression; +/-, partial expression; dim+, weak expression; and ++, strong expression. *, $P<0.05$.

intracellular FCM analyses were performed on cryopreserved cell suspensions of two BCL2-mutated samples, both demonstrating detectable BCL2 protein expression (**Figure 3D**).

Diffuse large B cell lymphoma (DLBCL)

DLBCL showed a significantly higher mean FSC signal than normal lymphocyte populations (121.84±9.17 vs. 102.09±11.58, P<0.05), indicating that DLBCL cells are larger in size (**Figure 4A**). These cells also exhibited monotypic expression of cKappa or cLambda, with strong or positive CD45 expression. CD19 was expressed in all cases, with one case showing strong expression and the other cases showing positive or weak expression. Antigens such as CD20, CD5, CD22, CD79b, CD71, CD200, FMC7, CD43, CD23, CD11c, CD81, CD25, sIgD, CD123, sIgM, CD8, CD38, and CD274 showed various expression patterns (positive, weak, partial, or negative); antigens that were consistently absent included CD10, CD3, CD56, CD103, and CD4 (**Figure 4B**). Mutations in the BCL6 (5/13) and KMT2D (4/13) genes were the most common in DLBCL (**Figure 4C**). We also detected a partial expression of BCL6 protein in a stored BCL6-mutated sample by intracellular staining (**Figure 4D**).

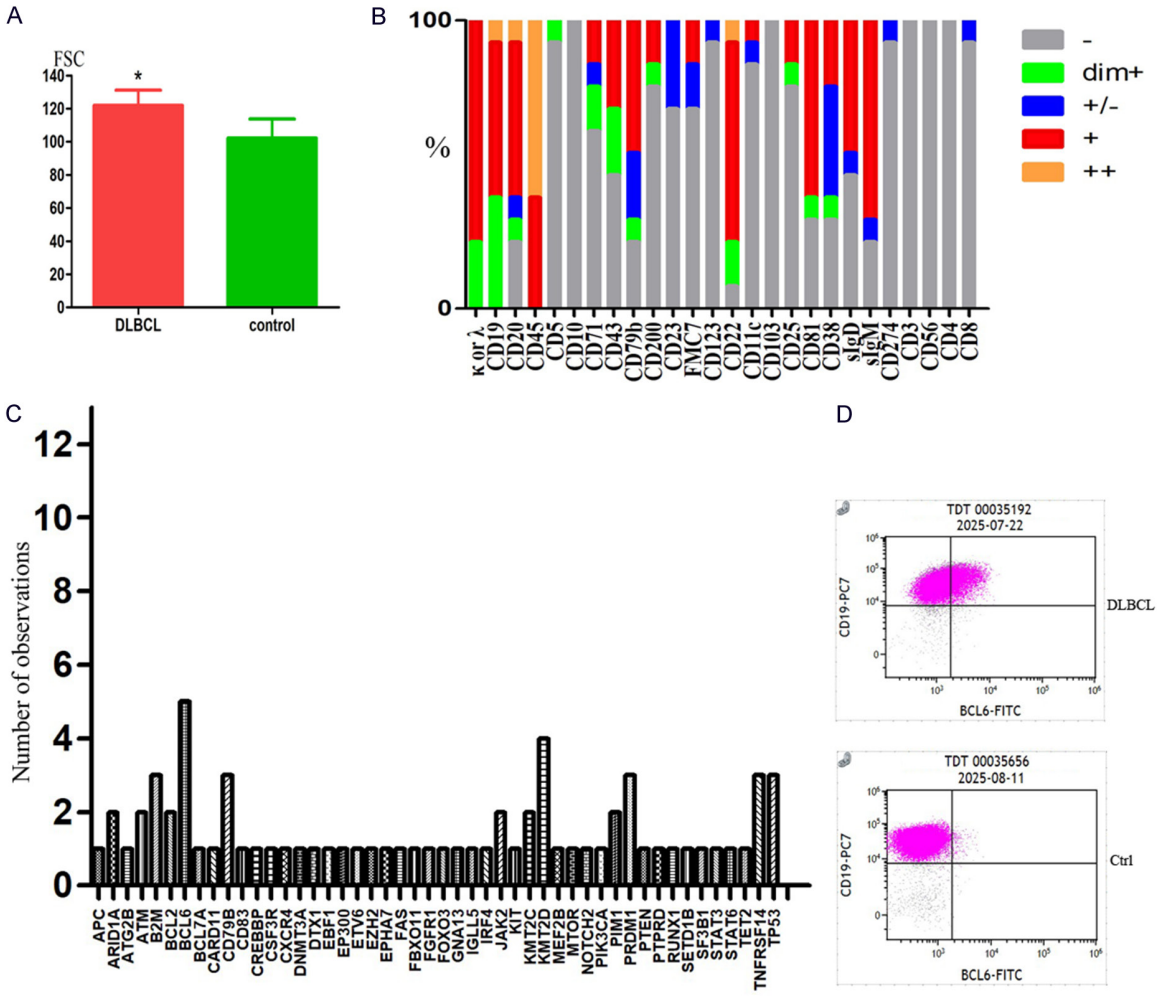

Figure 4. Flow cytometric analysis of antigen expression profiles in 13 DLBCL lymph node samples. A. Average FSC signal from B cells in the DLBCL and control groups. B. Immunophenotypic features of BCL cells in 13 DLBCL lymph node samples. C. Analysis of gene mutations in 13 DLBCL samples. D. BCL-6 expression in DLBCL by FCM. DLBCL, diffuse large B-cell lymphoma; FSC, forward scatter. -, negative expression; +, positive expression; +/-, partial expression; dim+, weak expression; and ++, strong expression. *, $P<0.05$.

MCL, MZL, and other BCL

Four cases of MCL, two of MZL and six other unclassifiable BCLs were detected. All these lymphomas demonstrated cell sizes smaller than that of control lymphocytes (Supplementary Figure 2A) and cells exhibited monotypic expression of kappa or lambda. CD45 showed strong or positive expression, while CD19 showed positive or weak positive expression. In MCL, CD5 was positive and CD10 was negative. In MZL, CD5 and CD10 were both negative. In the six cases of other lymphomas, CD10 was negative. However, further immunophenotypic features could not be detected due to the small sample sizes (Supplementary Figure 2B-D).

Identification of abnormal T cells by FCM

Lymphocytes were identified in the CD45 vs. SSC scatter plot. Then, gating was performed using CD3 vs. CD2, CD3 vs. CD5, CD3 vs. CD7, and CD4 vs. CD8 scatter plots to identify abnormal T lymphocytes (**Figure 5A**). FCM testing revealed 11 patients with T- and NK-cell lymphoma, including T-ALL/LBL (5 cases), AITL (1 case), ALCL (1 case), PTCL (2 cases), NK/T-cell lymphoma (1 case), and MF (1 case). All samples showed enhanced, attenuated, partial, or negative expression of CD2, CD3, CD5, CD7, or CD45, while two samples also showed abnormal CD56 expression (**Figure 5B**; Supplementary Table 2). In six samples, neither CD4 nor

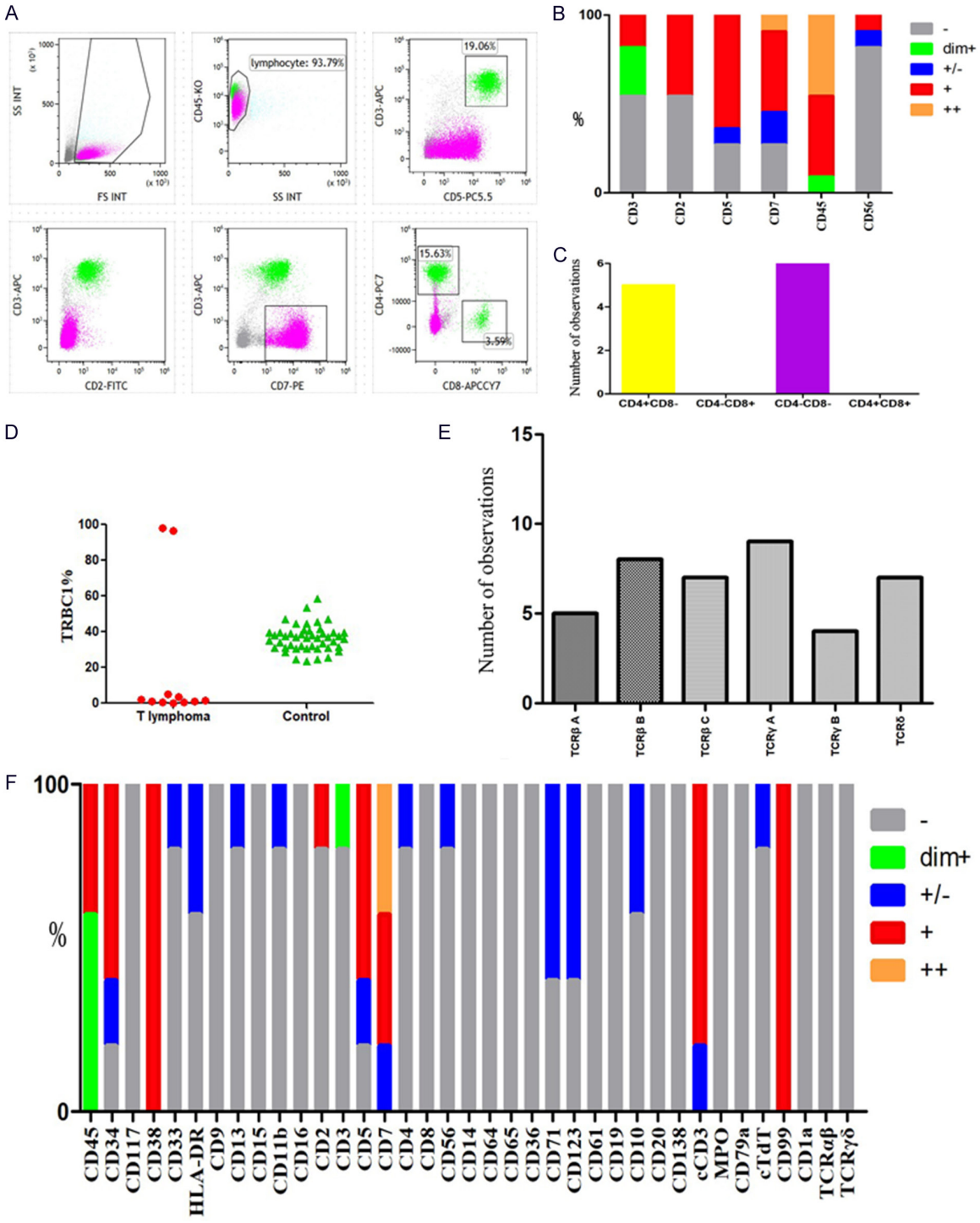

Figure 5. Screening of abnormal T cells in lymph node samples. A. T lymphocytes are labeled green, and abnormal cell populations are labeled purple. The abnormal cell populations showed strong CD7 expression, positive CD45 expression, partial CD5 expression, no CD2 or CD3 expression, and double negative expression for CD4 and CD8. B. Common expression patterns of CD2, CD3, CD5, CD7, CD45, and CD56 in 11 T- and NK-cell lymphoma lymph node samples. C. CD4 and CD8 expression in 11 T- and NK-cell lymphoma samples: CD4, but not CD8, expression in 5 cases (yellow), and double negative CD4 and CD8 expression in 6 samples (purple). D. The expression of TRBC1 in T lymphoma. E. Detection of TCR (T Cell Receptor) gene rearrangement. F. Flow cytometric analysis of antigen expression profiles in 5 T-ALL/LBL lymph node samples. T-ALL/LBL, T-cell acute lymphoblastic leukemia and lymphoblastic lymphoma. -, negative expression; +, positive expression; +/-, partial expression; dim+, weak expression; and ++, strong expression.

CD8 were expressed by abnormal T cells; the remaining five samples showed expression of CD4 but not CD8 (**Figure 5C**).

The TRBC1 expression was elevated in two T-cell lymphoma samples (97.9% and 96.4%), while the TRBC1 expression was 1.17%±1.61% in the other 9 samples. The expression of TRBC1 in T-cell lymphoma exceeded the normal range we recognized, which was 15%-85% (36.60%±7.21% in the control group) (**Figure 5D**). TCR gene rearrangements were detected in all samples, with the rearrangements of the TCRγ A (9/15) and TCRβ B (8/15) being the most common (**Figure 5E**).

T-ALL/LBL

The five T-ALL/LBL samples each exhibited unique FCM immunophenotype. CD45 expression was dim to moderate, in contrast to its strong expression on normal mature T lymphocytes. The CD2, CD3, CD5, or CD7 antigens showed strong, weak, partial, or no expression in all samples. One case showed CD4 but not CD8 expression, whereas the other four cases were negative for CD4 and CD8 (Supplementary Table 2). CD99 and CD38 were positive in all samples; CD3 and CD7 were also positive in all samples but showed various intensity (strong, positive, or partial). Antigens such as CD34, CD33, HLA-DR, CD13, CD11b, CD2, CD3, CD4, CD5, CD56, CD71, CD123, CD10, and cTdT showed positive, weak, partial, or no expression; antigens that were consistently absent included CD117, CD9, CD15, CD16, CD8, CD14, CD64, CD65, CD36, CD61, CD19, CD20, CD138, MPO, CD79a, CD1a, TCRαβ, and TCRγδ (**Figure 5F**).

Discussion

Lymphoma is a highly heterogenous hematologic malignancy that requires a multi-modal diagnostic approach for accurate classification [20, 21]. While histopathology remains the gold standard, multi-parameter FCM serves as an effective adjunct [5, 6]. This study was built on prior work showing that single-cell suspensions of intact lymph node tissues provides adequate cellularity and immunologic integrity, enabling comprehensive antigen profiling, a crucial benefit over FNA [17, 22].

A primary aim of this study was to determine the diagnostic value of FCM performed on intact lymph node tissue. The concordance between FCM and histopathologic examination in the detection of lymphoma was excellent (100% specificity and 100% PPV), which is consistent with the high concordance rates reported by earlier studies of Demurtas et al. [17] and Colorado et al. [20]. This is further supported by the Cohen Kappa of 0.72, which reflects a substantial level of concordance, reinforcing that FCM is a highly reliable and selective tool when used on the intact lymph nodes.

Additionally, our comprehensive immunophenotyping of BCL confirmed several well-established diagnostic profiles. For example, CLL/SLL cells exhibited reduced FSC signals (smaller size) and a typical CD5+/CD200+/CD10- profile, fully consistent with the known diagnostic criteria [9, 11] and large-scale immunophenotyping investigations [20]. Similarly, the FL cells also exhibited a smaller size than normal B-cells and showed the expected germinal center phenotype (CD10+/CD5-). In contrast, DLBCL cells featured a much higher FSC signal (greater size). These results are in line with the established morphologic and immunophenotypic continuum of BCL and underscore that FCM can offer objective, quantitative parameters (such as FSC) that correspond well with histopathologic findings.

An important observation in the tumor microenvironment was the significantly elevated PD-1 expression on T cells in BCL patients, particularly in DLBCL. This observation aligns with a previous finding of a high expression of PD-1 on follicular helper T (Tfh) cells in BCL. The possible underlying mechanism is the formation of an immunosuppressive and lymphoma-supportive microenvironment, in which the interaction of PD-1 with its ligand (PD-L1) - also detected on T cells in our study - suppressed T-cell effector functions and facilitates immune escape by the lymphoma [23, 24]. These data further support the biological rationale for PD-1/PD-L1 blockade therapies in lymphoma.

Despite these insights, our study revealed a limitation in the sensitivity (78.9%) of FCM. MCM missed 15 lymphoma cases (including two DLBCLs and several T-cell lymphomas). We attribute the difference, particularly in BCL, to possible sampling error. Additionally, as a retrospective study, selection bias regarding sample availability for both NGS and FCM may have influenced the detection rates.

In the cases of T- and NK-cell lymphoma, diagnostic challenges were even more pronounced. Our FCM identified 11 cases, which was less than the 15 cases identified by pathological examination. This difference was probably due to incomplete marker coverage for certain subtypes or sampling errors. Nevertheless, the 11 samples identified all demonstrated aberrant expression (loss of pan-T-cell antigens such as CD2, CD3, CD5 or CD7) and abnormal CD4/CD8 ratios. The results are consistent with the reports of Karube et al. [25] and others [26, 27]. Additionally, our TRBC1 analysis supported the diagnostic value of FCM for T-cell clonality. We observed a clear clonal restriction, with TRBC1 expression either >96% or <2%, consistent with the patterns described by Berg et al. [28], and Horna et al. [14].

We have also corroborated the long-established shortcomings of FCM in the diagnosis of classical Hodgkin lymphoma (HL) and metastatic cancer. These diagnoses are difficult to detect by FCM due to the rarity and fragility of Hodgkin/Reed-Sternberg (RS) cells [29] and the absence of specific hematopoietic markers in metastatic tumors. We failed to identify the single HL case and detected only 1 metastatic case, underscoring the inherent constraints of FCM in these diagnostic contexts [29, 31].

The most innovative aspect of our study was the integration of genetic data to guide immunophenotyping. The mutation profiles we identified wre highly consistent with the genetic abnormalities that underpin contemporary lymphoma classification [32]. The high prevalence of BCL2 and EZH2 mutations in FL, and BCL6 and KMT2D mutations in DLBCL, confirm that our cohort reflects the typical genetic landscapes for these diseases as defined by the WHO classification.

Building on this, we retrospectively validated a "mutation-guided" diagnostic loop based on this direct genotype-phenotype correlation. Our study successfully demonstrated the feasibility of this approach: BCL-2 protein expression was detected by FCM in BCL2-mutated FL samples and BCL-6 protein in a BCL6-mutated DLBCL sample. While IHC remains the traditional method, our findings suggest FCM can serve as a rapid, quantitative, and complementary method to confirm that a detected mutation is functionally expressed at the protein level. We acknowledge the small number of cases tested in this pilot - an unavoidable limitation related to sample preservation - but the results still support future investigation of this strategy.

Conclusion

FCM on intact lymph nodes is a highly specific and reliable method for lymphoma immunophenotyping, with excellent performance metrics (100% Specificity, 100% PPV) and substantial agreement (κ=0.72) with the gold standard. We have validated its use in characterizing B- and T-cell lymphomas, from cell size (FSC) to specific antigen profiles. Most importantly, we have provided proof-of-concept for an integrated "mutation-guided" workflow, linking NGS data to protein-level expression by FCM. This integrated, multi-parameter strategy refines lymphoma classification and enhances diagnostic accuracy.

Acknowledgements

This study was supported by grants from the Natural Science Foundation of Fujian Province (grant No. 2021J011397) and Quanzhou Science and Technology Project (grant No. 2022NS053).

Disclosure of conflict of interest

None.

Address correspondence to: Chun-Tuan Li, Department of Hematology, Quanzhou First Hospital of Affiliated to Fujian Medical University, Quanzhou 362000, Fujian, China. E-mail: lct070707@163.com

References

[1] GBD 2019 Stroke Collaborators. Global, regional, and national burden of stroke and its risk factors, 1990-2019: a systematic analysis for the global burden of disease study 2019. Lancet Neurol 2021; 20: 795-820.

[2] Liu Y, Chu Y, Liu J, Ge X, Ding M, Li P, Liu F, Zhou X and Wang X. Incidence and mortality of second primary malignancies after lymphoma: a population-based analysis. Ann Med 2023; 55: 2282652.

[3] Wang J, Young L, Win W and Taylor CR. Distribution and ZAP-70 expression of WHO lymphoma categories in Shanxi, China: a review of 447 cases using a tissue microarray technique. Appl Immunohistochem Mol Morphol 2005; 13: 323-32.

[4] Mugnaini EN and Ghosh N. Lymphoma. Prim Care 2016; 43: 661-75.
[5] Stetler-Stevenson M. Flow cytometry in lymphoma diagnosis and prognosis: useful? Best Pract Res Clin Haematol 2003; 16: 583-97.
[6] Shumilov E, Mazzeo P, Zinkernagel MS, Legros M, Porret N, Romagna L, Haase D, Lenz G, Novak U, Banz Y, Pabst T and Bacher U. Comprehensive laboratory diagnostic workup for patients with suspected intraocular lymphoma including flow cytometry, molecular genetics and cytopathology. Curr Oncol 2022; 29: 766-76.
[7] Trindade CJ, Sun X, Maric D, Sharma S, Komarow HD, Hourigan CS, Klion A and Maric I. Flow cytometric immunophenotypic differentiation patterns of bone marrow eosinophilopoiesis. Cytometry B Clin Cytom 2024; 106: 370-82.
[8] Hoeller S, Zhou Y, Kanagal-Shamanna R, Xu-Monette ZY, Hoehn D, Bihl M, Swerdlow SH, Rosenwald A, Ott G, Said J, Dunphy CH, Bueso-Ramos CE, Lin P, Wang M, Miranda RN, Tzankov A, Medeiros LJ and Young KH. Composite mantle cell lymphoma and chronic lymphocytic leukemia/small lymphocytic lymphoma: a clinicopathologic and molecular study. Hum Pathol 2013; 44: 110-21.
[9] Kroft SH and Harrington AM. Flow cytometry of B-cell neoplasms. Clin Lab Med 2017; 37: 697-723.
[10] Debord C, Wuillème S, Eveillard M, Theisen O, Godon C, Le Bris Y and Béné MC. Flow cytometry in the diagnosis of mature B-cell lymphoproliferative disorders. Int J Lab Hematol 2020; 42 Suppl 1: 113-20.
[11] Yuan CM, Vergilio JA, Zhao XF, Smith TK, Harris NL and Bagg A. CD10 and BCL6 expression in the diagnosis of angioimmunoblastic T-cell lymphoma: utility of detecting CD10+ T cells by flow cytometry. Hum Pathol 2005; 36: 784-91.
[12] Wang JC, Deng XQ, Liu WP, Gao LM, Zhang WY, Yan JQ, Ye YX, Liu F and Zhao S. Comprehensive flow-cytometry-based immunophenotyping analysis for accurate diagnosis and management of extranodal NK/T cell lymphoma, nasal type. Cytometry B Clin Cytom 2020; 98: 28-35.
[13] Muñoz-García N, Morán-Plata FJ, Villamor N, Lima M, Barrena S, Mateos S, Caldas C, van Dongen JJM, Orfao A and Almeida J. High-sensitive TRBC1-based flow cytometric assessment of T-cell clonality in tαβ-large granular lymphocytic leukemia. Cancers (Basel) 2022; 14: 408.
[14] Horna P, Shi M, Olteanu H and Johansson U. Emerging role of T-cell receptor constant β chain-1 (TRBC1) expression in the flow cytometric diagnosis of T-cell malignancies. Int J Mol Sci 2021; 22: 1817.
[15] Morice WG, Kurtin PJ, Hodnefield JM, Shanafelt TD, Hoyer JD, Remstein ED and Hanson CA. Predictive value of blood and bone marrow flow cytometry in B-cell lymphoma classification: comparative analysis of flow cytometry and tissue biopsy in 252 patients. Mayo Clin Proc 2008; 83: 776-85.
[16] Ensani F, Mehravaran S, Irvanlou G, Aghaipoor M, Vaeli S, Hajati E, Khorgami Z and Nasiri S. Fine-needle aspiration cytology and flow cytometric immunophenotyping in diagnosis and classification of non-hodgkin lymphoma in comparison to histopathology. Diagn Cytopathol 2012; 40: 305-10.
[17] Demurtas A, Stacchini A, Aliberti S, Chiusa L, Chiarle R and Novero D. Tissue flow cytometry immunophenotyping in the diagnosis and classification of non-Hodgkin's lymphomas: a retrospective evaluation of 1,792 cases. Cytometry B Clin Cytom 2013; 84: 82-95.
[18] Tbakhi A, Edinger M, Myles J, Pohlman B and Tubbs RR. Flow cytometric immunophenotyping of non-hodgkin's lymphomas and related disorders. Cytometry 1996; 25: 113-24.
[19] Cheah CY and Seymour JF. Marginal zone lymphoma: 2023 update on diagnosis and management. Am J Hematol 2023; 98: 1645-57.
[20] Colorado M, Cuadrado MA, Insunza A, Mazorra F, Acinas O and Iriondo A. Simultaneous cytomorphologic and multiparametric flow cytometric analysis on lymph node samples is faster than and as valid as histopathologic study to diagnose most non-Hodgkin lymphomas. Am J Clin Pathol 2010; 133: 83-91.
[21] Ferry JA. Scientific advances and the evolution of diagnosis, subclassification and treatment of lymphoma. Arch Med Res 2020; 51: 749-64.
[22] Jin X, Jiang H, Jiang Y, Chen Z, Zhou W, Pan Q and Tian S. Analysis of flow cytometry data from ultrasound-guided lymph node biopsies with two types of needles. Int J Lab Hematol 2024; 46: 869-77.
[23] Huang YH, Wan CL, Dai HP and Xue SL. Targeted therapy and immunotherapy for T cell acute lymphoblastic leukemia/lymphoma. Ann Hematol 2023; 102: 2001-13.
[24] Heming M, Haessner S, Wolbert J, Lu IN, Li X, Brokinkel B, Müther M, Holling M, Stummer W, Thomas C, Schulte-Mecklenbeck A, de Faria F, Stoeckius M, Hailfinger S, Lenz G, Kerl K, Wiendl H, Meyer Zu Hörste G and Grauer OM. Intratumor heterogeneity and T cell exhaustion in primary CNS lymphoma. Genome Med 2022; 14: 109.
[25] Karube K, Satou A and Kato S. New classifications of B-cell neoplasms: a comparison of 5th WHO and international consensus classifications. Int J Hematol 2025; 121: 331-41.

[26] You MJ, Medeiros LJ and Hsi ED. T-lymphoblastic leukemia/lymphoma. Am J Clin Pathol 2015; 144: 411-22.
[27] Aussedat G, Fontaine J, Gerland LM, Traverse-Glehen A and Baseggio L. Lymphoma diagnosis: lessons learned from the comparison of histology and cytology associated with flow cytometry. Ann Biol Clin (Paris) 2022; 80: 157-68.
[28] Berg H, Otteson GE, Corley H, Shi M, Horna P, Jevremovic D and Olteanu H. Flow cytometric evaluation of TRBC1 expression in tissue specimens and body fluids is a novel and specific method for assessment of T-cell clonality and diagnosis of T-cell neoplasms. Cytometry B Clin Cytom 2021; 100: 361-9.
[29] Jiang M, Bennani NN and Feldman AL. Lymphoma classification update: T-cell lymphomas, hodgkin lymphomas, and histiocytic/dendritic cell neoplasms. Expert Rev Hematol 2017; 10: 239-49.
[30] Fromm JR, Kussick SJ and Wood BL. Identification and purification of classical hodgkin cells from lymph nodes by flow cytometry and flow cytometric cell sorting. Am J Clin Pathol 2006; 126: 764-80.
[31] Grewal RK, Chetty M, Abayomi EA, Tomuleasa C and Fromm JR. Use of flow cytometry in the phenotypic diagnosis of hodgkin's lymphoma. Cytometry B Clin Cytom 2019; 96: 116-27.
[32] Jaffe ES. Diagnosis and classification of lymphoma: impact of technical advances. Semin Hematol 2019; 56: 30-6.

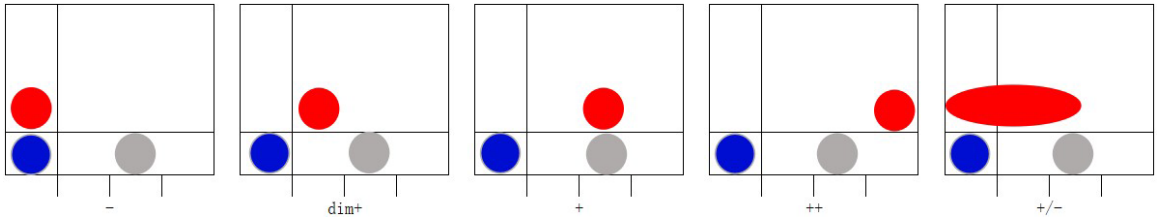

Supplementary Figure 1. Representative flow cytometric plots defining antigen expression levels. This figure illustrates the criteria used to classify antigen expression based on the percentage of positively labeled cells and fluorescence intensity. Antigen expression is categorized as follows: Negative (-): positive cell population ≤15%; Partial (+/-): positive cell population between 15% and 70%; Positive (+): positive cell population ≥70%. Among positive populations (≥70%), expression is further classified as Weak (dim+): fluorescence intensity lower than the positive control, or Strong (++): fluorescence intensity higher than the positive control.

Supplementary Table 1. B cell lymphoma panel by next generation sequencing and TCR gene rearrangement

Lymphoma	Panel									
B	APC	ARID1A	ATG2B	ATM	B2M	BCL2	BCL6	BCL7A	CARD11	CCND3
	CD58	CD79A	CD79B	CD83	CREBBP	CSF3R	CXCR4	D13S25	DNMT3A	DTX1
	EBF1	EP300	ETV6	EZH2	EPHA7	FAT1	FANCD2	FANCM	FBXW7	FOXO1
	FAS	FBXO11	FGFR1	FOXO3	GNA13	IGLL5	IGH	IGHV	IRF4	ITGA4
	JAK2	JAK3	KIT	KLHL6	KMT2C	KMT2D	MEF2B	MTOR	MYBBP1A	MYC
	NOTCH1	NOTCH2	PIK3CA	PIM1	PRDM1	PTEN	PTPRD	RB1	RHOA	RUNX1
	SETD1B	SETD2	SF3B1	SOCS1	SPEN	STAT3	STAT6	TET2	TMSB4X	TNFRSF14
	TP53	TRAF3								
T	TCRβ A	TCRβ B	TCRβ C	TCRγ A	TCRγ B	TCRδ				

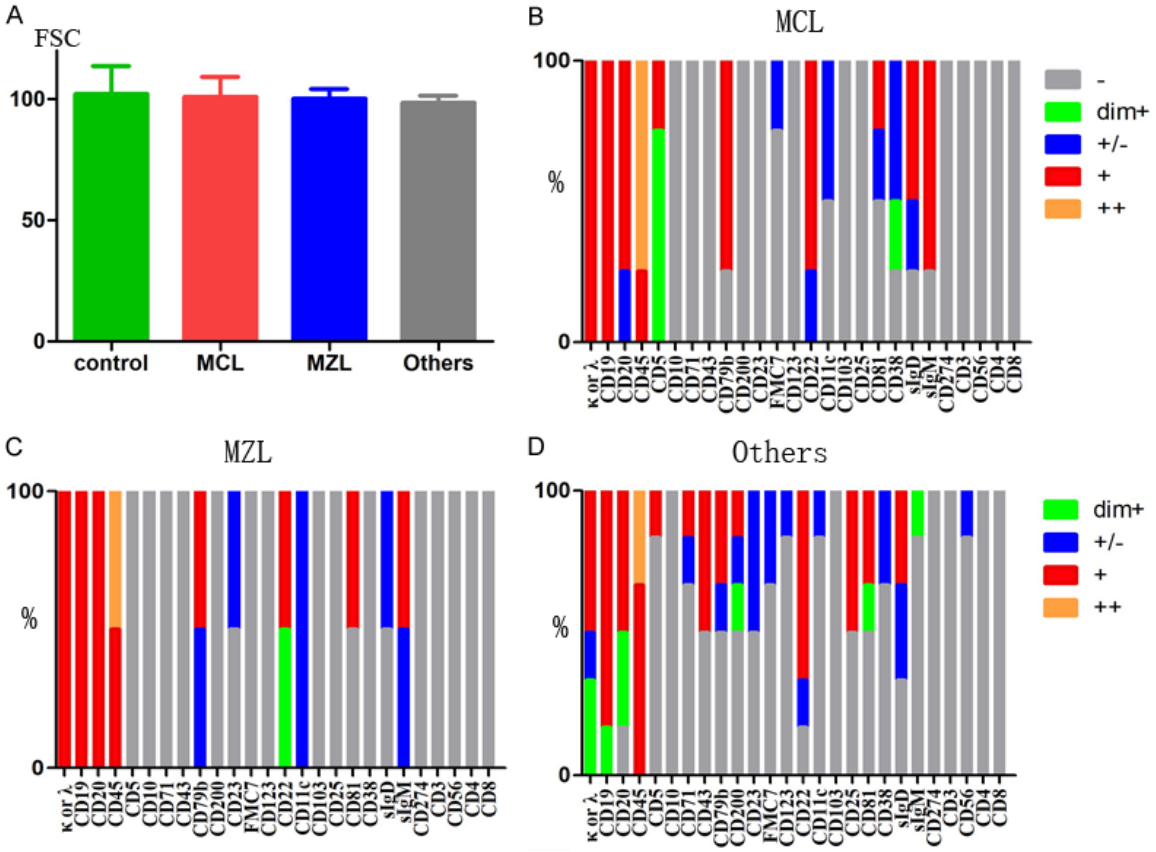

Supplementary Figure 2. RImmunophenotypic profiles and cell size analysis of MCL, MZL, and other B-cell lymphomas. A. Comparison of Forward Scatter (FSC) signals, representing cell size, among Control (normal B-cells), Mantle Cell Lymphoma (MCL), Marginal Zone Lymphoma (MZL), and other unclassified B-cell lymphoma groups. Data are presented as mean ± SD. B. Stacked bar charts showing the percentage of antigen expression intensity in 4 MCL cases. C. Antigen expression profiles for 2 MZL cases. D. Antigen expression profiles for 6 other unclassified B-cell lymphomas. The color keys indicate expression levels: gray (-) indicates negative expression; green (dim+) indicates weak expression; blue (+/-) indicates partial expression; red (+) indicates positive expression; and orange (++) indicates strong expression.

Supplementary Table 2. Antigen expression in T-cell lymphoma lymph node samples

	Diagnosis	CD3	CD2	CD5	CD7	CD56	CD45
patinet1	T-ALL/LBL	dim+	+	+	+	-	+
patinet2	MF	dim+	-	-	-	-	++
patinet3	PTCL	-	+	+	+/-	-	++
patinet4	AITL	-	+	+	+	-	++
patinet5	T-ALL/LBL	-	-	+	+/-	+/-	+
patinet6	AITL	+	+	+	-	-	++
patinet7	PTCL	dim+	+	+	+	-	++
patinet8	T-ALL/LBL	-	-	+	++	-	+
patinet9	NK/T cell lymphoma	+	-	-	-	+	+
patinet10	T-ALL/LBL	-	-	-	+	-	dim+
patinet11	T-ALL/LBL	-	-	+/-	++	-	+